

Implementation of Electrochemically Synthesized Silver Nanocrystallites for the Preferential SERS Enhancement of Defect Modes on Thermally Etched Graphite Surfaces

Jim V. Zoval, Peter R. Biernacki, and Reginald M. Penner*

Institute for Surface and Interface Science, Department of Chemistry, University of California, Irvine, California 92715-2025

Highly oriented pyrolytic graphite (HOPG) surfaces, on which atomically well-defined roughness has been introduced via high-temperature gasification reactions, are investigated by noncontact mode atomic force microscopy (NC-AFM) and Raman spectroscopy both before and after the electrochemical deposition of silver nanocrystallites on these surfaces. Exposure of freshly cleaved HOPG surfaces to an O₂-rich ambient at 650 °C for a few minutes caused the formation of 1-monolayer-deep, circular etch pits on the HOPG basal plane surface. Silver nanocrystallites were electrochemically deposited onto these etched surfaces at two coverages: 0.5 mC cm⁻² (or 5 nmol of Ag⁰ cm⁻²) and 2.4 mC cm⁻² (25 nmol of Ag⁰ cm⁻²). At the lower coverage, NC-AFM images revealed that silver decorated only the circumference of the circular etch pits, forming a uniform annular ring with an apparent diameter of 200–250 Å and a height of ~15 Å. At the higher silver coverage, an increase in the height but not the diameter of this annulus was observed, and additional silver nanostructures—having dimensions of 300–350 Å diameter and 15 Å height—were observed on atomically smooth regions of the graphite basal plane. The Raman spectroscopy of these surfaces was investigated and compared with spectra for nanocrystallite-modified but unetched HOPG basal plane surfaces and thermally etched surfaces on which no silver was deposited. For thermally etched HOPG surfaces at either silver coverage, SERS-augmented Raman spectra were obtained in which defect modes of the graphite surface—derived from “finite” graphite domains at the surface—were strongly and preferentially enhanced. In addition, an enhanced band near 2900 cm⁻¹ was assigned to ν_{OH} from carboxylate moieties present at step edges based on the basis of the observed pH dependence of the enhancement.

The primary purpose of this paper is to demonstrate the utility of silver nanocrystallites, electrocrystallized on graphite surfaces using a recently described technique,¹ for the enhancement of Raman modes of surface defects. Previously, two strategies have been employed to acquire surface-enhanced Raman spectra (SERS) for functionalities or adsorbates which are intrinsic to non-SERS-active metals. The first strategy, described by Weaver and

co-workers,^{2–6} involves the electrochemical deposition—by underpotential deposition (UPD)—of mono- or bilayers of non-SERS-active metals (e.g., Pt, Ru, Rh) on electrochemically roughened gold surfaces. Because the distance separating the surface of the non-SERS-active metal from the SERS-active gold surface in these experiments can be as small as 1 metal monolayer (<5 Å), strong electromagnetic enhancement of the Raman signal for adsorbates (such as carbon monoxide^{4,6}) at the metal overlayer has been observed in these experiments.

A second, complementary strategy which accomplishes the same objective involves the decoration of the non-SERS-active metal surface with a SERS-active metal. In this case, it is intended to employ a silver deposit as a nonintrusive amplifier of Raman-active modes which are intrinsic either to the clean metal surface or to molecules specifically adsorbed on this surface. Van Duyne and Haushalter⁷ described the first implementation of this strategy in 1983, involving the electrochemical deposition of small amounts of silver onto gallium arsenide (GaAs) surfaces. The intent in this experiment was to amplify the Raman signal of tris(bipyridyl)-ruthenium(II) specifically adsorbed at the GaAs(100) surface.⁷ Subsequently, Pemberton employed this strategy to probe platinum electrodes surfaces on which silver had been electrodeposited,⁸ and in several more recent studies,^{9–12} the SERS of various carbon electrode surfaces on which silver has been deposited either by hot filament evaporation or by electrochemical deposition have been investigated. Particularly relevant to this paper are the Raman spectroscopic investigations of silver-modified carbon electrodes (including HOPG, pyrolytic graphite, and glassy carbon) by Alsmeyer and McCreery published in 1991 and 1992.^{9,13} These spectroscopic studies—which involved graphite surfaces that were immersed in electrolyte solutions and maintained under potential control—tracked the SERS spectrum as a function of the

- (2) Desilvestro, J.; Corrigan, D. A.; Weaver, M. J. *J. Phys. Chem.* **1986**, *90*, 6408.
- (3) Desilvestro, J.; Corrigan, D. A.; Weaver, M. J. *J. Electrochem. Soc.* **1988**, *135*, 885.
- (4) Leung, L.-W. H.; Weaver, M. J. *J. Am. Chem. Soc.* **1987**, *109*, 5113.
- (5) Leung, L.-W. H.; Weaver, M. J. *J. Electroanal. Chem.* **1987**, *217*, 367.
- (6) Leung, L.-W. H.; Weaver, M. J. *Langmuir* **1988**, *4*, 1076.
- (7) Van Duyne, R. P.; Haushalter, J. P. *J. Phys. Chem.* **1983**, *87*, 2999.
- (8) Pemberton, J. E. *J. Electroanal. Chem.* **1984**, *167*, 317.
- (9) Alsmeyer, Y. W.; McCreery, R. L. *Langmuir* **1991**, *7*, 2370.
- (10) Alsmeyer, Y.-W.; McCreery, R. L. *Anal. Chem.* **1991**, *63*, 1289.
- (11) Ishida, H.; Fukuda, H.; Katagiri, G.; Ishitani, A. *Appl. Spectrosc.* **1986**, *40*, 322.
- (12) Rubim, J. C.; Kannen, G.; Schumacher, D.; Dünnwald, J.; Otto, A. *Appl. Surf. Sci.* **1989**, *37*, 233.
- (13) Alsmeyer, D. C.; McCreery, R. L. *Anal. Chem.* **1992**, *64*, 1528.

(1) Zoval, J.; Stiger, R.; Biernacki, P.; Penner, R. M. *J. Phys. Chem.* **1996**, *100*, 837.

quantity of electrochemically deposited silver. For glassy carbon, pyrolytic graphite, and HOPG electrodes, Alsmeyer and McCreery demonstrated a strong and selective enhancement of the surface disorder-induced D band following electrochemical silver deposition at electrodes that were subjected to either electrochemical or laser pretreatment procedures.^{9,13} On glassy carbon surfaces, silver coverages up to $0.30 \mu\text{mol cm}^{-2}$ were probed. A maximum SERS enhancement of the D mode was observed for a silver coverage of $0.20 \mu\text{mol cm}^{-2}$ (or ~ 70 equivalent monolayers), and the minimum silver coverage, corresponding to the onset of SERS enhancement of the D mode, was reported to be $\sim 3.5 \text{ mC cm}^{-2}$ or 10 equivalent silver monolayers.¹⁰

In the present work, a recently described potentiostatic pulse electrochemical method¹ has been employed to deposit silver nanocrystallites onto basal plane-oriented graphite surfaces which possess atomically well-defined roughness in the form of 1–2 monolayer-deep, circular etch pits.^{14–22} NC-AFM images of thermally treated HOPG revealed the formation of a high density ($\sim 10^8$ – 10^9 cm^{-2}) of circular etch pits, each 500–2000 Å in diameter and 3–4 Å in depth, on the graphite surface, as previously reported.^{14–18,20–22} Despite the increased density of surface defects generated by this thermal treatment, Raman spectra of thermally treated and unmodified HOPG surfaces were nearly identical. These surfaces were then probed by Raman spectroscopy and by NC-AFM following the deposition of silver at two different coverages: 0.50 and 2.4 mC cm^{-2} , corresponding to 1.4 and 6.8 equivalent silver monolayers, respectively. Collectively, the data obtained demonstrate the following: (i) Silver “amplifier” particles, which are very nearly of an optimal diameter for generating strong electromagnetic enhancement of Raman signals (for reviews, see refs 23 and 24), are readily obtained by pulsed potentiostatic deposition at graphite surfaces. (ii) At low Coulombic loadings, corresponding to 5 nmol of $\text{Ag}^0 \text{ cm}^{-2}$ (approximately 1.4 equivalent monolayers), silver nucleates and grows preferentially at edge defect sites on the HOPG surface. SERS enhancement of the Raman-active modes associated with these defects was clearly obtained with minimum enhancement factors, EF_{min} , for the $1579 \text{ cm}^{-1} \text{ E}_{2\text{g}}$ mode estimated to be ~ 140 . (iii) The location of silver nuclei on the graphite surface can readily be made more uniform (and the deposition, therefore, less defect-selective) by increasing the quantity of silver deposited. With coulometric loadings of $\sim 2.4 \text{ mC cm}^{-2}$ (or ~ 6.8 equivalent monolayers), larger silver nuclei were observed at step edges, and 15–20% of the silver particles were located on defect-free regions of the graphite basal plane. Greater SERS enhancements for defect modes were observed at this higher silver coverage, with EF_{min} values of more than 300 for both the D (1392 cm^{-1}) and $\text{E}_{2\text{g}}$ modes of the surface. (iv) The observed SERS enhancements persists with slight diminution at silver-modified HOPG surfaces exposed to air for at least 2 h.

- (14) Chang, H.; Bard, A. J. *J. Am. Chem. Soc.* **1991**, *113*, 5588.
 (15) Chang, H.; Bard, A. J. *J. Am. Chem. Soc.* **1990**, *112*, 4598.
 (16) Chu, X.; Schmidt, L. D. *Carbon* **1991**, *29*, 1251.
 (17) Chu, X.; Schmidt, L. D. *Surf. Sci.* **1992**, *268*, 325.
 (18) Chu, X.; Schmidt, L. D.; Chen, S. G.; Yang, R. T. *J. Catal.* **1993**, *140*, 543.
 (19) Pakula, T.; Tracz, A.; Wegner, G.; Rabe, J. P. *J. Chem. Phys.* **1993**, *99*, 8162.
 (20) Siperko, L. M. *J. Vac. Sci. Technol. B* **1991**, *9*, 1061.
 (21) Atamny, F.; Schlögl, R.; Wirth, W. J. *Ultramicroscopy* **1992**, *42*, 660.
 (22) Patrick, D. L.; Cee, V. J.; Beebe, T. P. *Science* **1994**, *265*, 231.
 (23) Kerker, M. *Acc. Chem. Res.* **1984**, *17*, 271.
 (24) Moskovits, M. *Rev. Mod. Phys.* **1985**, *57*, 783.

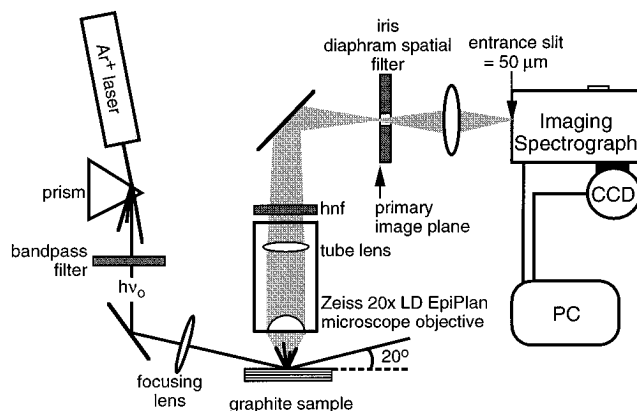


Figure 1. Schematic diagram of the home-built Raman microprobe instrument used for the experiments described in this paper.

EXPERIMENTAL SECTION

Highly oriented pyrolytic graphite of unspecified grade was obtained from Advanced Ceramics Inc. The pitted graphite surfaces that are of interest in this study were prepared by heating a freshly cleaved basal plane surface in flowing O_2 in a tube furnace at $650 \text{ }^\circ\text{C}$ for 2–3 min, as previously described.^{14–16,18} These conditions produced circular etch pits on the HOPG surface that were 1 or 2 monolayers in depth and 500–2000 Å in diameter.

The electrochemical deposition of silver followed a previously published procedure,¹ except that larger quantities of silver were deposited in these experiments. Briefly, electrochemical silver deposition was performed in a Kel-F cell in which an O-ring exposed a circular region ($A = 0.1062 \text{ cm}^2$) of the graphite surface to a N_2 -sparged plating solution of aqueous 1.0 mM silver nitrate (Johnson Matthey, 99.9%) and 0.10 M potassium nitrate (Fisher >99.95%). This solution was prepared using Nanopure water ($\rho > 18 \text{ M}\Omega$). The potentiostatic deposition of silver was accomplished using a silver wire reference electrode and a platinum wire counter electrode. Silver deposition was effected by stepping the potential of the graphite surface to -100 mV using a Bioanalytical Systems CV-27 potentiostat. The coulometric loading of silver (either 2.4 or 0.5 mC cm^{-2}) was taken to be the charge integrated from the onset of this potential step. Following silver deposition, the graphite electrode surface was rinsed with Nanopure water and dried in an oven at $60 \text{ }^\circ\text{C}$. Except for the time dependence study, Raman spectra were acquired for each surface within 15 min of the deposition of silver.

Noncontact AFM experiments were performed using a Park Scientific Instruments (PSI Inc.) AutoProbe cp instrument equipped with the noncontact head. This instrument operates in the slope-detected mode.^{25,26} Cantilevers were $2.0\text{-}\mu\text{m}$ -thick silicon nitride Microlevers (PSI Inc.) having a force constant, specified by the manufacturer, of 0.15 N/m , a resonance frequency near 300 kHz , and a nominal tip radius of 100 \AA . The amplitude of the cantilever diather was $\sim 5 \text{ \AA}$ far from the surface and $1\text{--}2 \text{ \AA}$ during imaging. All imaging experiments were performed in the laboratory air ambient.

SERS spectra were acquired using the Raman microprobe instrument shown in the schematic diagram of Figure 1. Excita-

- (25) Albrecht, T. R.; Grütter, P.; Horne, D.; Rugar, D. *J. Appl. Phys.* **1991**, *69*, 668.
 (26) Lüthi, R.; Meyer, E.; Howald, L.; Haefke, H.; Anselmetty, D.; Dreier, M.; Rüetschi, M.; Bonner, T.; Overnewy, R. M.; Frommer, J.; Güntherodt, H.-J. *J. Vac. Sci. Technol. B* **1994**, *12*, 1673.

tion from a Coherent Innova 90-6 argon ion laser operating at 5145 Å (TEM 00) and focused to a beam diameter of 0.8 mm was incident on the graphite surface at an angle of 80° from surface normal (external to the collection optics) in the laboratory air ambient. Scattered light from the surface was collected at normal incidence using a 20× Zeiss EpiPlan objective. Rayleigh scatter was eliminated from this signal using a holographic notch filter (Kaiser Notch-Plus), and the inelastically scattered residual was coupled with an *f*/4 lens into an imaging spectrograph (Chromex 250IS, equipped with a 1200 grooves mm⁻¹ holographic grating; 500 nm blaze) that dispersed the light onto a liquid nitrogen-cooled CCD (Princeton Instruments Model LN/1024EUV) having 1024 × 256 pixels. Signals from the 256 pixels arrayed perpendicular to the long axis of the CCD were binned, producing a linear detector with 1024 channels. In conjunction with the linear dispersion produced by the 1200 grooves mm⁻¹ grating, the pixel-wise resolution of this detector was 1.6 cm⁻¹.

The spectrograph was calibrated using the emission lines of a mercury lamp. This calibration was verified two ways: first, ν_{N_2} and ν_{O_2} modes at 2345 and 1555 cm⁻¹, respectively, were present in every spectrum, and second, two additional calibration points at the high- and low-energy extremes of the relevant spectral region were periodically verified using prominent chloroform modes at 1221 and 3032 cm⁻¹. A relatively long collection time of 350 s, necessitated by the low numerical aperture of the long-working-distance 20× objective, was employed for laser powers of 400–450 mW. To facilitate comparison of the peak intensities for the various spectra across variations in the laser power and possible illumination nonuniformities at the sample, the Raman band for N₂ was employed to normalize all spectra to that of spectrum E in Figure 6. In addition, all spectra were subjected to the cosmic ray removal algorithm of the Princeton software.

RESULTS AND DISCUSSION

NC-AFM of HOPG Surfaces. In a small but growing number of studies,^{26–29} the noncontact atomic force microscope (NC-AFM) has been successfully employed to probe the topography of labile surfaces that are difficult to successfully image using either scanning tunneling microscopy or atomic force microscopy—including metal nanoparticles.²⁷ Like the conventional atomic force microscope (AFM), the NC-AFM (or dynamic force microscope) operates by measuring and maintaining a small force between a sharp probe tip and the sample surface which is imaged, while the tip is scanned in a raster pattern across the sample surface. However, whereas the AFM tip interacts repulsively with the sample surface, the NC-AFM tip is positioned in the *attractive* region of the tip–surface interaction potential—at distances from the surface of more than 10–15 Å. The potential gradient (or force) sampled at these distances is much smaller than the repulsive force gradients existing closer to the surface, and the detection of this gradient is accomplished by dithering the probe tip in the direction perpendicular to the sample surface, with an amplitude of ~1–2 Å and a frequency near the cantilever resonance. This amplitude is smaller than that normally employed to obtain stable images of a surface using the related intermittent contact (IC) or “tapping” AFM imaging modes. Phase-sensitive

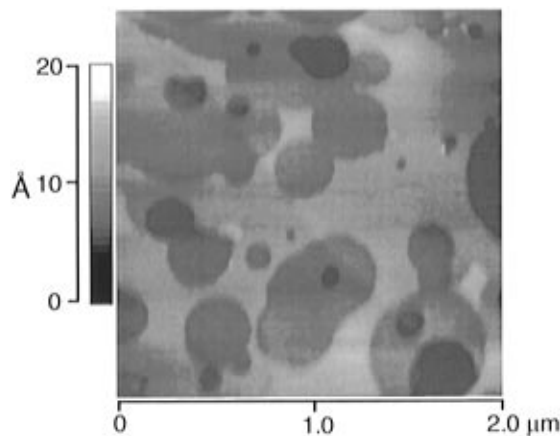


Figure 2. NC-AFM image of typical HOPG surface after heating in flowing O₂ at 650 °C for 3 min. The circular pits produced by gasification reactions of the graphite surfaces are evident in this image.

detection is employed to measure the damping of the probe's amplitude caused by the drag exerted by the attractive tip–surface interaction. The feedback circuit of the microscope acts on the amplitude-damping signal to maintain the sample at a distance that preserves the potential gradient, and therefore the tip–sample distance, at some preset value as the tip is scanned slowly (typically at ~1–2 Hz) across the sample surface.

A representative NC-AFM image of an HOPG surface that was heated in flowing O₂ at 650 °C for 3 min is shown in Figure 2. It is now well-established^{14–22} that, under these conditions, gasification reactions of the graphite surface lead to layer-by-layer etching of the basal plane surface. From point sites of initiation on the atomically smooth graphite basal plane, the gasification reaction progresses radially while remaining confined to a single graphite layer leading to the formation of circular etch pits that are 1 graphite monolayer, or 3.3 Å, in depth. These etch pits, having a typical depth of 1 graphite monolayer or 3.3 Å, are obvious in the NC-AFM image of Figure 2.

Onto etched surfaces like that shown in Figure 2, and pristine graphite surfaces, silver was deposited by the pulsed potentiostatic method using a pulse amplitude of 100 mV vs. Ag⁰/Ag⁺ and a pulse duration as required to yield either of two Coulombic loadings for silver: 0.5 or 2.4 mC cm⁻². Following the deposition of 0.5 mC cm⁻² of silver metal (corresponding to 5 nmol of Ag cm⁻² or 1.4 equivalent monolayers) onto the thermally treated HOPG surfaces, NC-AFM images like that shown in Figure 3 were obtained. These surfaces appear to be topographically similar to the clean thermally treated HOPG surfaces shown in Figure 2, except that in Figure 3A and B, each etch pit is surrounded by a raised annulus having an apparent width of 300–350 Å and a height of ~10 Å (see cross section, Figure 3C). For graphite surfaces on which 2.4 mC cm⁻² of silver was deposited (corresponding to 20 nmol of Ag cm⁻² or 6.8 equivalent monolayers), the NC-AFM images of Figure 4A and B reveal that the annular silver deposit associated with the circumference of pits became beaded in appearance, with the height fluctuating between 20 and 30 Å about the circumference of a typical etch pit (see cross section, Figure 4C). In addition, many “free-standing” silver nuclei having apparent dimensions of 300–350 Å diameter and 20–25 Å height were observed on defect-free regions of the graphite basal plane. It is important to emphasize that, at pristine graphite surfaces that were not thermally treated to generate pits, we have

(27) Schaefer, D. M.; Patil, A.; Andres, R. P.; Reifenberger, R. *Appl. Phys. Lett.* **1993**, *63*, 1492.

(28) McIntire, T. M.; Penner, R. M.; Brant, D. A. *Macromolecules* **1995**, *28*, 6375.

(29) Anselmetti, D.; Dreier, M.; Lüthi, R.; Richmond, T.; Meyer, E.; Frommer, J.; Güntherodt, H.-J. *J. Vac. Sci. Technol. B* **1994**, *12*, 1500.

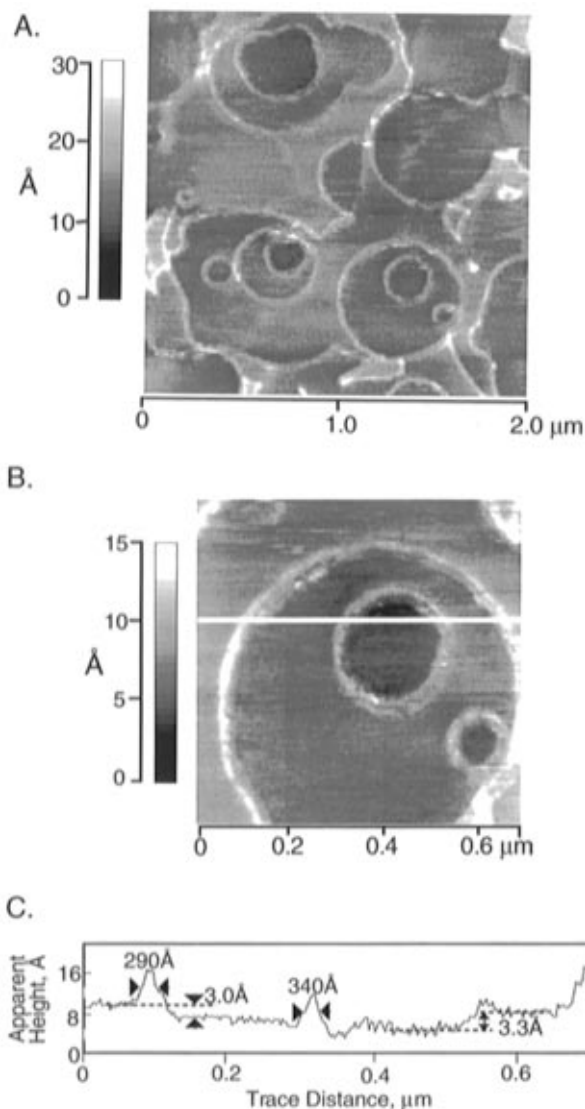


Figure 3. (A) NC-AFM image of thermally pitted HOPG with electrodeposited Ag along step edges of the pits. $Q_{Ag} = 0.5 \text{ mC cm}^{-2}$ (or $5 \text{ nmol of Ag}^0 \text{ cm}^{-2}$). (B) A higher magnification image of the same surface. (C) Amplitude trace acquired along the indicated line in Figure 3B.

previously shown that, for the deposition of much smaller quantities of silver—from 0.040 to $40.0 \mu\text{C cm}^{-2}$ (or 0.4 to $400 \text{ pmol of Ag}^0 \text{ cm}^{-2}$)—a uniform coverage of silver nanocrystallites is produced for which individual particles are similar in size to those shown in Figure 4.¹ Based on this observation, a tentative conclusion is that the electrochemical deposition of silver at both pristine and thermally treated surfaces proceeds by the preferential decoration of step edges, followed by the electrocrystallization of silver at defect-free regions of the graphite surface, and that at thermally treated graphite surfaces, saturation of step edges with a silver annulus occurs at Coulombic loadings which are nearly 3 orders of magnitude higher than those at the pristine graphite basal plane.

For purposes of comparison, silver was also electrochemically deposited at the higher coverage of 2.4 mC cm^{-2} onto pristine basal plane graphite surfaces. As shown in the NC-AFM image of Figure 5A, a high coverage of $\sim 10^{10} \text{ cm}^{-2}$ of silver particles is associated with defect-free regions of the graphite basal plane surface, as previously reported.¹ On pristine basal plane graphite surfaces, we have shown¹ that, in addition to the nanocrystallites

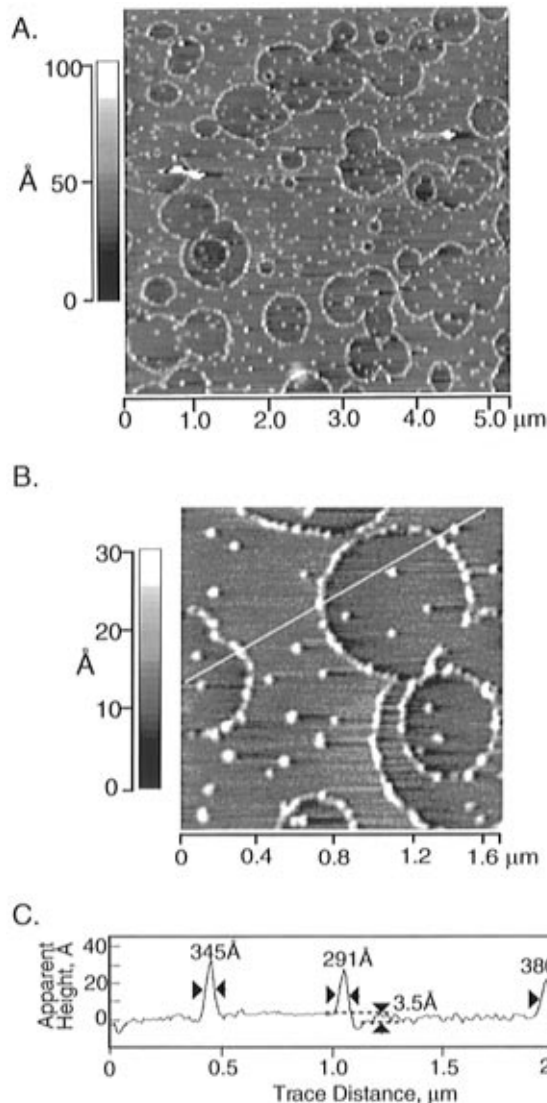


Figure 4. (A) NC-AFM image of thermally pitted HOPG with electrodeposited Ag along the step edges of the pits. $Q_{Ag} = 2.4 \text{ mC cm}^{-2}$ (or $25 \text{ nmol of Ag}^0 \text{ cm}^{-2}$). (B) Higher magnification image of the same surface. (C) Amplitude trace acquired along the line indicated in Figure 3B.

shown in Figure 5A, a population of silver *micro*crystallites which are ~ 100 times as large as the nanocrystallites of Figure 5A are also present at Coulombic loadings greater than $15 \mu\text{C cm}^{-2}$. None of these larger silver particles are present in the image of Figure 5A.

The cross sections shown in Figures 3C, 4C, and 5B all indicate that the apparent diameter of the electrochemically deposited silver particles (300 – 500 Å) was larger by a factor of ~ 20 as compared with the height of ~ 10 – 20 Å . This diameter–height asymmetry was observed for silver particles in all the NC-AFM experiments conducted in connection with this paper, and in previous work.¹ We have also seen a similar effect for NC-AFM experiments involving single polysaccharide chains on mica surfaces—in cross section, these chains appear to be ~ 6 – 10 Å in height and 200 – 300 Å in diameter.²⁸ It is now well-appreciated that the *apparent* diameter of protrusions that are rendered with an AFM contains a contribution from the geometry of the AFM probe tip. Because long-range interactions are important in the NC-AFM experiment, the nature of the tip convolution is more complicated than for repulsive mode AFM. Height measurements

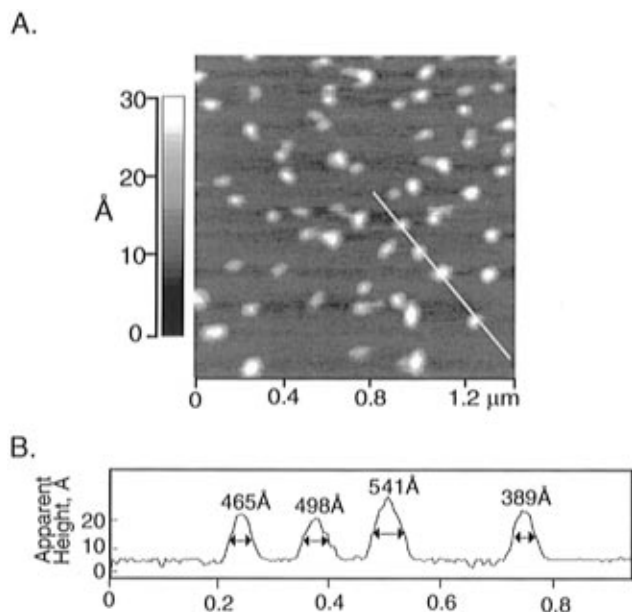


Figure 5. (A) NC-AFM images of Ag electrodeposited onto the pristine basal plane surface of HOPG. $Q_{Ag} = 2.4 \text{ mC cm}^{-2}$. (B) Amplitude trace acquired along the line indicated in Figure 5A.

of nanostructures, in contrast, are comparatively accurate, since this measurement is insensitive to the precise AFM probe tip geometry. In the specific case of electrochemically deposited silver particles on graphite, transmission electron micrographs of silver particles transferred to TEM grids reveal that these particles are approximately spherical and possess diameters consistent with the NC-AFM-apparent height to within $\pm 10\%$.¹

Raman Spectroscopy. In Figure 6 are shown Raman scattering survey spectra for the energy range from 1200 to 3200 cm^{-1} . Five spectra are shown corresponding to freshly cleaved and unmodified graphite (A), thermally etched graphite onto which no silver was deposited (B), freshly cleaved graphite onto which 2.4 mC cm^{-2} of silver was deposited generating silver nanostructures (C), and thermally etched graphite onto which 0.5 and 2.4 mC cm^{-2} of silver was deposited (D and E, respectively). The intensities of each spectrum in Figure 6 have been normalized to the N_2 stretching vibration of Figure 6A to compensate for variations of the laser intensity at the sample surface, and the indicated sensitivity is specific to spectrum A.

Thermally etched and pristine HOPG surfaces (Figure 6A,B) yielded identical Raman scattering spectra. These spectra, which are dominated by the E_{2g} mode at 1581 cm^{-1} and a doublet in the second-order Raman spectrum with peaks at ~ 2700 and 2730 cm^{-1} , are entirely consistent with the spectrum for HOPG reported in many previous studies. Consistent with the reported results of Alsmeyer and McCreary,¹⁰ the deposition of silver onto pristine HOPG surfaces yielded spectra (Figure 6C) which were substantially the same as those for clean HOPG. In general, however, we observed a new and relatively weak band near 2930 cm^{-1} , the origin of which is discussed below. However, in the spectra of Figure 6D and E obtained following the deposition of silver onto thermally treated surfaces, the emergence of new modes at 1280, ~ 1392 , and 2938 cm^{-1} is apparent. In addition, at the higher silver coverage, the scattering intensity of the preexisting mode at 1581 cm^{-1} is increased substantially. A further discussion of the five spectra shown in Figure 6 focuses first on the interval from 1200 to 1700 cm^{-1} , which includes the E_{2g} phonon mode or G mode

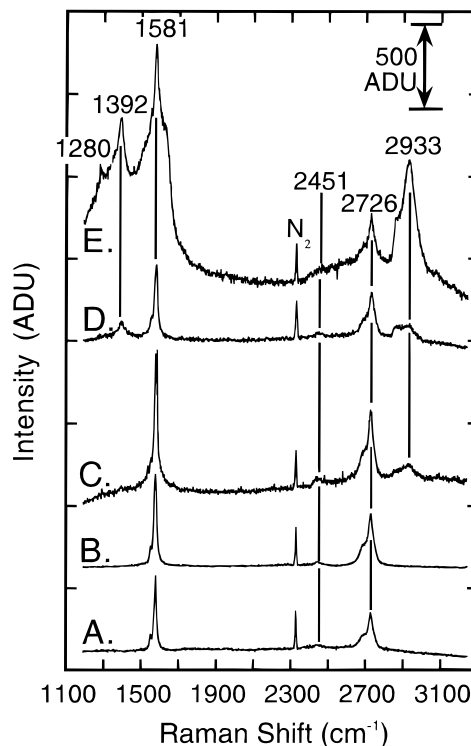


Figure 6. Raman scattering survey spectra encompassing 1200–3200 cm^{-1} : (A) pristine HOPG, no silver; (B) thermally etched HOPG, no silver; (C) pristine HOPG, $Q_{Ag} = 2.4 \text{ mC cm}^{-2}$ (or 25 nmol of $\text{Ag}^0 \text{ cm}^{-2}$); (D) thermally etched HOPG, $Q_{Ag} = 0.5 \text{ mC cm}^{-2}$ (or 5 nmol of $\text{Ag}^0 \text{ cm}^{-2}$); (E) thermally etched HOPG, $Q_{Ag} = 2.4 \text{ mC cm}^{-2}$ (or 25 nmol of $\text{Ag}^0 \text{ cm}^{-2}$). All five spectra were normalized using the N_2 intensity of spectrum A.

at $\sim 1581 \text{ cm}^{-1}$ characteristic of defect-free graphite, the D mode, usually observed at 1360 cm^{-1} , and the D' mode near 1630 cm^{-1} .³⁰ The second spectral region considered is that from 2600 to 3100 cm^{-1} , which encompasses the second-order (i.e., two photon) phonon modes located at 2726³¹ and $\sim 2930 \text{ cm}^{-1}$.

Spectral Region: 1200–1700 cm^{-1} . Previous studies have established that defectiveness of the graphite surface is indicated by three distinct spectral signatures in this wavelength regime. First, the existence and intensity of two peaks—at 1360 (the D band) and 1620 cm^{-1} (the D' band)—have been widely employed^{9–13,20,30–39} to quantitate the degree of surface defectiveness. Tuinstra and Koenig,^{30,39} for example, have observed that the ratio of the D to the G bands was inversely proportional to the microcrystallite size, L_a . The origin of the 1360 cm^{-1} band is disputed,⁴⁰ however, a peak in the phonon density of states exists at this energy,⁴¹ and on the basis of this fact and experimental data, McCreary and co-workers⁴⁰ have presented convincing

(30) Tuinstra, F.; Koenig, J. L. *J. Chem. Phys.* **1970**, *53*, 1126.

(31) Nemanich, R. J.; Solin, S. A. *Phys. Rev. B* **1979**, *20*, 392.

(32) Dillon, R. O.; Woollam, J. A.; Katkanant, V. *Phys. Rev. B* **1984**, *29*, 3482.

(33) Elman, B. S.; Dresselhaus, M. S.; Dresselhaus, G.; Maby, E. W.; Mazurek, H. *Phys. Rev. B* **1981**, *24*, 1027.

(34) Elman, B. S.; Shayegan, M.; Dresselhaus, M. S.; Mazurek, H.; Dresselhaus, G. *Phys. Rev. B* **1982**, *25*, 4142.

(35) Lee, E. H.; Hembree, D. M.; Rao, G. R.; Mansur, L. K. *Phys. Rev. B* **1993**, *48*, 15540.

(36) Knight, D.; White, W. B. *J. Mater. Res.* **1989**, *4*, 385.

(37) Nakamura, K.; Fuitsuka, M.; Kitajima, M. *Chem. Phys. Lett.* **1990**, *172*, 205.

(38) Nakamura, K.; Kitajima, M. *Phys. Rev. B* **1992**, *45*, 78.

(39) Tuinstra, F.; Koenig, J. L. *J. Comput. Math.* **1970**, *4*, 492.

(40) Wang, Y.; Alsmeyer, D. C.; McCreary, R. L. *Chem. Mater.* **1990**, *2*, 557.

(41) Al-Jishi, R.; Dresselhaus, G. *Phys. Rev. B* **1982**, *26*, 4514.

arguments that the 1360 cm^{-1} band is a first-order phonon mode which is symmetry forbidden at infinite graphite surfaces, but which becomes active with the relaxation of wave vector conservation caused by the interruption of the smooth basal plane surface by defects such as step edges or substitutional impurities. Second, surface disorder-induced line broadening of the E_{2g} peak at $\sim 1580\text{ cm}^{-1}$ has been reported by Nakamura et al.⁴² The origin of this line broadening is postulated to be an increase in the uncertainty of the wavevector, Δq , by an amount $2\pi/L_a$, caused by the existence of finite graphite domains with dimension L_a on the surface. A linear increase of the line width from 16 to 70 cm^{-1} was observed on the interval of $2\pi/L_a$ from 0 to 0.2 \AA^{-1} , corresponding to $L_a > 30\text{ \AA}$.⁴² Finally, shifts of the E_{2g} band to higher energy (and less frequently to lower energy) have been correlated with a decrease in L_a .³⁷

Freshly cleaved graphite surfaces exhibited none of these three spectral indicators of damage, irrespective of the presence of silver on the surface, and spectra for naked (Figure 6A) and silver-modified surfaces (Figure 6C) were identical. The apparent insensitivity of the Raman spectrum to the thermally induced damage visible in the NC-AFM images of Figure 2, however, is easily rationalized: The etch pits generated by the thermal treatment are confined to the outer-most graphite atomic layer (i.e., $\sim 3.5\text{ \AA}$), while the penetration depth of the $\lambda = 5145\text{ \AA}$ laser light at HOPG has been estimated to be 125 \AA , or approximately 38 graphite atomic layers, at the angle of incidence of 80° employed in these experiments.¹⁰

Thermally pitted surfaces on which no silver was deposited exhibited no D band at $\sim 1360\text{ cm}^{-1}$. However, with the deposition of silver at the lower coverage, a new band near 1392 cm^{-1} was usually observed. At the higher silver coverage probed in the spectrum of Figure 6E, this band has emerged as the second strongest in the spectrum after the E_{2g} at 1581 cm^{-1} . It should be noted that, in other experiments, the spectral region between 1350 and 1550 cm^{-1} exhibited some variability with bands in addition to the 1392 cm^{-1} band sometimes present (cf. spectra shown in Figure 8). The origin of the 1392 cm^{-1} mode is, at first, somewhat puzzling. It is improbable that this band is assignable to the A_{1g} mode (i.e., the D band) based on two considerations. First, in many previous Raman spectroscopic investigations of graphite surfaces in which the surface has been roughened using a variety of methods (ion implantation,^{32–35,38} laser irradiation and anodization,^{9,43} e-beam irradiation,^{37,42} etc.), the D band has consistently been observed in the range from 1355 to 1360 cm^{-1} , 30 cm^{-1} lower than its observed position in these experiments. Second, it is well established that the overtone of A_{1g} band is observed in the second-order Raman spectrum near 2720 cm^{-1} —even in spectra of the unmodified HOPG basal plane. This band (which is half of a doublet having a characteristic envelope) is present at approximately the expected energy, 2726 cm^{-1} , in each of the spectra shown in Figure 6. This fact leads immediately to the conclusion that the 1392 cm^{-1} band cannot be the fundamental from which the 2726 cm^{-1} band is derived.

The energy of the 1392 cm^{-1} band does, however, correspond to a peak in the density of states (at the M -point) for a single graphite layer in the lattice dynamical mode for graphite proposed by Laspade, Al-Jishi, and Dresselhaus.^{41,44} This same in-plane

phonon mode has been invoked by Rubim et al.¹² to explain the observation of a 1391 cm^{-1} mode as a shoulder on the more intense 1360 cm^{-1} D mode in SERS spectra of glassy carbon. In contrast to the results of Rubim et al., however, we did not observe the D band at 1360 cm^{-1} in many separate experiments involving thermally etched graphite surfaces. It is therefore concluded that—for reasons which are as yet unclear—graphite surfaces possessing atomic scale roughness of the type generated by the thermal annealing procedure provide an excellent opportunity for the observation and study of this unusual phonon mode of the surface.

Also present in the spectrum of Figure 6E is a shoulder on the high-energy side of the E_{2g} band at $\sim 1630\text{ cm}^{-1}$. This feature has been termed the D' band, and its presence is linked with the existence of surface defects in several previous studies. Its presence in the spectrum of the high silver coverage surface coincides with the emergence of the 1392 cm^{-1} mode at similar intensity. Neither of the two other spectral indicators of defectiveness listed above is present in the spectra of Figure 6C, D, or E: the line width of the E_{2g} band is 18 cm^{-1} , which was in the range from 16 to 18 cm^{-1} typically observed for this peak at the full range of graphite surfaces probed in this study. This range of line widths is actually narrower than the minimum observed for defect-free graphite surfaces ($\sim 22\text{ cm}^{-1}$) in the study by Nakamura et al.⁴²

Regarding the effect of electrochemically deposited silver nanostructures on the first-order Raman spectra of etched and pristine graphite surfaces, the following conclusions apply: (1) Except for some variation in the intensities of modes, the Raman spectrum of freshly cleaved graphite (with and without silver) and thermally etched graphite samples without silver are identical. (2) Modes at 1392 and 1630 cm^{-1} are strongly and preferentially enhanced following the electrochemical deposition of silver on etched HOPG surfaces at the higher silver coverage of 2.4 mC cm^{-2} . At the lower silver coverage investigated, a lesser degree of enhancement is evident for the 1392 cm^{-1} band, and the band at 1630 cm^{-1} is absent. (3) Although linked to the existence of the monoatomic step edges produced by thermal etching, it is unlikely that the 1392 cm^{-1} band observed in this study has the same origin as that proposed previously for the 1360 cm^{-1} or D mode. Instead, this mode likely derives from another peak in the density of states for a single graphite layer.

Spectral Region: 2600 – 3100 cm^{-1} . This spectral region encompasses the second-order Raman scattering spectrum for graphite which, in the phonon density of states calculations of Al-Jishi and Dresselhaus,⁴¹ is dominated by two peaks near 2700 and 2730 cm^{-1} . Experimentally, these peaks have frequently been observed as a doublet in which the 2700 cm^{-1} peak appears as a shoulder on the higher energy band;³¹ in the spectra of Figure 6A and B, these two peaks are observed in an envelope having the characteristic line shape with peaks at ~ 2688 and 2726 cm^{-1} .

Previously, these bands have been observed to weaken and broaden as the defectiveness of the graphite surface is increased by ion implantation, for example.^{31,33,35} However, it is apparent that these two second-order peaks are essentially unaffected by thermal etching, even for graphite surfaces on which silver nanostructures were deposited (Figure 6D,E). Instead, the evolution of this spectral region in Figure 6C,D is dominated by the emergence of two peaks at energies of 2856 and 2933 cm^{-1} . The 2856 cm^{-1} mode may be a combination band derived from

(42) Nakamura, K.; Fujitsuka, M.; Kitajima, M. *Phys. Rev. B* **1990**, *41*, 12260.

(43) Bowling, R. J.; Packard, R. T.; McCreery, R. L. *Langmuir* **1989**, *5*, 683.

(44) Laspade, P.; Al-Jishi, R.; Dresselhaus, G. *Carbon* **1982**, *20*, 427.

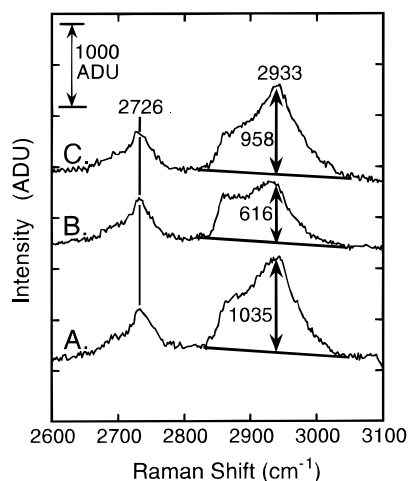


Figure 7. Raman scattering spectra of spectral region from 2600 to 3100 cm^{-1} . Spectrum A was acquired after silver electrodeposition ($Q_{\text{Ag}} = 2.4 \text{ mC cm}^{-2}$) at a thermally etched HOPG surface. This surface was then exposed to aqueous 10 mM KOH for 1 h (and air-dried) and spectrum B was acquired. Finally, the surface was reprotonated by exposure to aqueous 1 mM H_2SO_4 for 15 min and spectrum C was acquired.

Table 1. Relative Intensities and Minimum Enhancement Factors for Enhanced Raman Scattering Modes on Graphite Following Silver Nanocrystallite Deposition

silver coverage		1280 cm^{-1}	1392 cm^{-1}	1581 cm^{-1}	2933 cm^{-1}
5 nmol of $\text{Ag}^0 \text{ cm}^{-2}$	rel intens ^a	20	108	404	107
	min EF ^b	7	37	139	37
25 nmol of $\text{Ag}^0 \text{ cm}^{-2}$	rel intens ^a	612	897	1316	712
	min EF ^b	211	309	453	245

^a Relative intensity following normalization using the N_2 stretching mode. ^b Minimum enhancement factor calculated using eq 1 and $\sigma = 1.45$ counts from the spectrum of Figure 7B.⁴⁵

$1280 + 1581 \text{ cm}^{-1}$. This assignment is corroborated by the observed 3–4-fold increase in the intensity of this band caused by an increase in the silver coverage from 0.50 to 2.4 mC cm^{-2} , which also induces the emergence of the 1280 cm^{-1} mode in the spectrum (Figure 6E).

Assignment of the band at 2933 cm^{-1} is less clear-cut. One source for scattering intensity at this wavelength may be a combination band derived from the E_{2g} mode at $1581 + 1360 \text{ cm}^{-1}$. However, ν_{OH} , derived from carboxylates and alcohols present at terminations of a graphite layer, could constitute a second source of scattering intensity at this wavelength. To distinguish the component of the 2933 cm^{-1} mode derived from ν_{OH} of carboxylate from other possible sources of Raman spectroscopy scattering at this energy, this spectral region was probed by Raman following the deprotonation of etched graphite surfaces (having $Q_{\text{Ag}} = 2.4 \text{ mC cm}^{-2}$) in 10 mM aqueous KOH for 60 min. Prior to exposure to base, the spectrum of Figure 7A was collected; following exposure, Figure 7B was obtained. A 40% decrease in the intensity at 2933 cm^{-1} is readily apparent in this spectrum, whereas the adjacent peak at 2956 cm^{-1} is unaffected. Also, as expected for carboxylate, most of this intensity decrease was recoverable by subsequent reprotonation of surface acid sites by exposure of the surface to aqueous HCl (1.0 mM for 15 min; Figure 7C). The residual scattering intensity at 2933 cm^{-1} evident in the spectrum

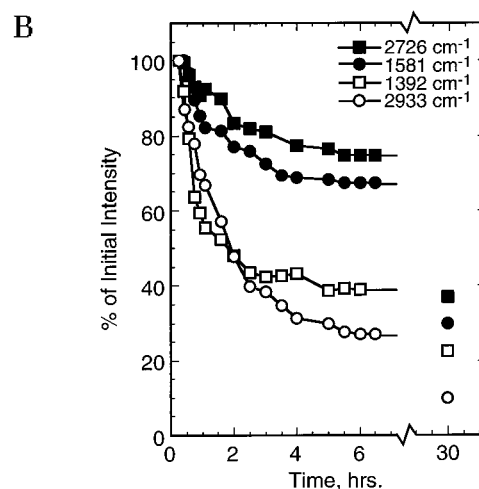
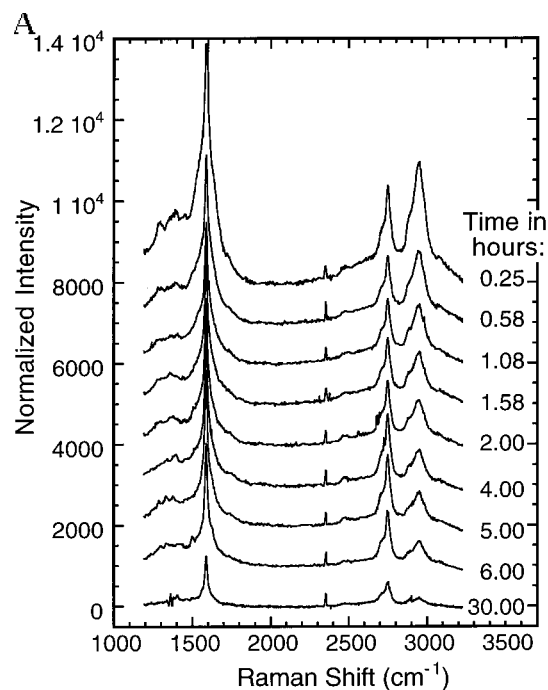


Figure 8. Representative time dependence of the Raman scattering spectra for an etched HOPG surface having $Q_{\text{Ag}} = 2.4 \text{ mC cm}^{-2}$ (or $25 \text{ nmol of Ag}^0 \text{ cm}^{-2}$) exposed to the laboratory air ambient. (A) Survey spectra acquired at the indicated intervals following silver electrodeposition ranging from 0.25 (top) to 30 h. (bottom). (B) Percentage of the initial scattering intensity (i.e., that observed at $t = 0.25 \text{ h}$) which is retained versus time for four peaks: 2726, 1581, 1391, and 2933 cm^{-1} .

of the deprotonated graphite surface (Figure 7B) likely derives both from combination bands and from nonacidic ν_{OH} and ν_{CH} at edge defect sites.

Minimum Enhancement Factors and Stability. The absolute magnitudes of the SERS enhancements for each of the bands are not easily quantitated since the bands affected by SERS at silver-modified surfaces were entirely absent from the spectra of Figure 6D and E obtained at silver-free surfaces. Although absolute enhancement factors are not readily estimated, it is possible to estimate the *minimum* enhancement factors, EF_{min} , which are referenced to the signal-to-noise ratio present in the unenhanced spectrum of Figure 6B. The relevant equation is

$$\text{EF}_{\text{min}} = I_{\text{peak}}/2\sigma \quad (1)$$

where 2σ represents the limit of detection of a scattering signal, estimated as twice the RMS noise in the spectrum of a thermally etched but clean HOPG surface of Figure 6B, and I_{peak} is the peak intensity following normalization. These EF_{min} values, which are tabulated in Table 1, range from 7 for the 0.5 mC cm^{-2} surface at 1280 cm^{-1} to 450 for the 2.4 mC cm^{-2} at 1581 cm^{-1} .⁴⁵ These EF_{min} values are very similar in magnitude to the enhancement factors estimated in the previous work of Alsmeyer and McCreery involving silver deposition on graphite and glassy carbon surfaces,¹⁰ despite the fact that the *maximum* quantity of deposited silver in this study (20 nmol cm^{-2} or 6.8 equivalent monolayers) was less than the *minimum* of 10 equivalent Ag monolayers required to observe the onset of a SERS enhancement at glass carbon surfaces in that earlier study. The implication is that the activity of the nanocrystalline silver deposit for producing an electronic enhancement of the Raman signal is greater than in previous studies.

The stability of the SERS enhancement observed at silver nanostructure-modified graphite surfaces exposed to air was probed by acquiring 15 spectra over a 30 h interval immediately following the deposition of fresh silver nanostructures onto graphite surfaces. In Figure 8A are shown typical spectra for a thermally treated HOPG surface having $Q_{\text{Ag}} = 2.4 \text{ mC cm}^{-2}$. The gradual diminution of the Raman scattering intensity for all bands in these spectra is readily apparent. As shown in the plot of peak intensities versus time of Figure 8B, the rate of decay was fastest during the first 2 h following deposition and most rapid for the D band at 1391 cm^{-1} and the 2938 cm^{-1} band, which retained just 25–40% of the intensity observed initially after 6 h in air. For the E_{2g} mode at 1581 cm^{-1} and the two overtone bands^{31,41} at 2763 cm^{-1} , in contrast, 70–80% of the initial scattering intensity was retained after 6 h. Further reductions in the intensities of all four peaks occurred over the ensuing 2 days, with peak intensities ranging from 40% (for 2743 cm^{-1}) to 10% (for 2938 cm^{-1}). The decay of the D' band at the 1630 cm^{-1} mode was difficult to quantitate because of its association with the more intense E_{2g} band. The spectrum observed following 30 h of air exposure is virtually indistinguishable from the spectrum for etched graphite surfaces on which no silver was deposited, shown in Figure 6B. Thus, it is concluded that processes such as air oxidation and the accumulation of a contamination layer effectively deactivate the silver deposit following a 30 h exposure to air.

SUMMARY

We have demonstrated that silver nanocrystallites deposited using a recently described method generate a strong SERS

(45) In other experiments, the observed EF_{min} values varied by about $\pm 10\%$ from those quoted in Table 1.

enhancement of defect modes of an HOPG surface on which atomic-scale roughness has been intentionally introduced. Silver coverages of $25 \text{ nmol of Ag}^0 \text{ cm}^{-2}$ (or ~ 6.8 equivalent monolayers) yielded enhancement factors of at least 450 for defect modes of thermally etched HOPG surfaces on which at most two atomic layers had been damaged. The onset of a SERS enhancement was readily apparent for a silver coverage of $5 \text{ nmol of Ag}^0 \text{ cm}^{-2}$. Degeneration of the SERS enhancement occurred with time following the electrochemical deposition of silver for surfaces that were continuously exposed to the laboratory air environment. For modes associated with surface defects (i.e., 1391 and 2933 cm^{-1}), the decay of the SERS enhancement with time was more rapid than for phonon modes associated with the bulk density of states of graphite.

The identity of the Raman modes observed for thermally etched surfaces differed appreciably from the most commonly observed modes reported in previous studies. In particular, the normally observed D mode at $\sim 1360 \text{ cm}^{-1}$ was replaced by a mode at 1391 cm^{-1} , which was strongly SERS enhanced. In addition, scattering at 2933 cm^{-1} was attributable to ν_{OH} on the basis of the observation of a pronounced intensity dependence of the scattering intensity at this energy with the state of protonation of the surface.

Previously we have demonstrated that the silver nanocrystallites generated by pulsed potentiostatic deposition interact very weakly with the HOPG basal plane and are removable.¹ It may, therefore, be possible to transfer and disperse silver nanocrystallites (prepared on HOPG surfaces) on other, non-SERS-active surfaces on which an electronic enhancement of the SERS signal is sought.

ACKNOWLEDGMENT

The financial support of this work was provided by grants from the Office of Naval Research (No. 400X119YIP) and the National Science Foundation (No. DMR-9257000). R.M.P. also acknowledges financial support as an A. P. Sloan Foundation Fellow, a Camille Dreyfus Teacher-Scholar, and a Young Investigator of the Arnold and Mabel Beckman Foundation. The authors express their gratitude to Mr. Art Moore of Advanced Ceramics Inc. for donation of some of the HOPG employed for these investigations, and to Park Scientific Instruments for the donation of some of the Microlevers employed for the NC-AFM imaging experiments.

Received for review November 10, 1995. Accepted February 13, 1996.[⊗]

AC951114+

[⊗] Abstract published in *Advance ACS Abstracts*, March 15, 1996.